CONF-970726--8

INVESTIGATION AND MODELING OF THE ELASTIC-PLASTIC FRACTURE BEHAVIOR OF CONTINUOUS WOVEN FABRIC-REINFORCED CERAMIC COMPOSITES

W. Keith Kahl
Oak Ridge National Laboratory
Engineering Technology Division
P.O. Box 2009 MS 8039
Oak Ridge, Tennessee 37831-8039
Ph: 423/574-0372
Fax: 423/574-9407
kahlwk@ornl.gov

ABSTRACT

The paper describes a study which attempted to extrapolate meaningful elastic-plastic fracture toughness data from flexure tests of a chemical vapor-infiltrated SiC / Nicalon fiber-reinforced ceramic matrix composite. Fibers in the fabricated composites were pre-coated with pyrolytic carbon to varying thicknesses. In the tests, crack length was not measured and the study employed an estimation procedure, previously used successfully for ductile metals, to derive J-R curve information. Results are presented in normalized load vs. normalized displacements and comparative J_{Ic} behavior as a function of fiber precoating thickness.

INTRODUCTION

In recent publications of work conducted at the Oak Ridge National Laboratory (ORNL) and the University of Tennessee, Knoxville (Miller, 1995; Lowden,1989; Miller et al.,1996), silicon carbide chemical vapor-infiltrated Nicalon fiber-reinforced ceramic composite material (CVI SiC-Nicalon) has been subjected to tensile, flexure, interlaminar shear and notched specimen fracture testing. The material was fabricated at ORNL and was prepared in several batches with different thicknesses of fiber coatings applied. The Nicalon fibers were precoated with a chemical vapor deposited (CVD) layer of pyrolytic graphite. Such coatings are employed to tailor desirable mechanical behavior at the fiber / matrix interface. Specifically, the presence of a buffering phase between the brittle matrix (SiC) and the fibers facilitates fiber debonding and pullout which bleeds energy from cracks advancing through the matrix. The net effect is a toughening mechanism which gives the bulk material a favorable characteristic of significant deformation prior to ultimate failure.

Miller (1995) sought to model the elastic behavior of this CVI-SiC material from load vs. displacement data gathered over multiple specimens subjected to unnotched 4-point bending tests and chevron-notched 3-point bending tests. The computational flow of the model considered increasing loads leading to stresses which caused matrix micro-cracking, then progressing to macro-crack extension through both phases. This linear elastic-based model employed beam theory and compliance matching schemes to generate "phantom" crack length and growth in unnotched modulus of rupture (MOR) bars. This permitted derivation of some K (linear elastic fracture toughness) values of interest. Miller also sought to generate predictive load-displacement curves as a function of fiber coating thickness.

Load-displacement data gathered in flexure testing of notched specimens of this material indicated "elastic-plastic like" behavior on a macroscopic scale. This prompted consideration of an alternate approach for describing the fracture mechanics of this ceramic matrix composite (CMC) material. It is postulated that useful engineering information can be derived from application of existing ductile fracture mechanics (elastic-plastic) as opposed to complicated models coupling many brittle processes (linear elastic). This paper presents results from a conventional *J-integral analysis* applied to CVI-SiC / Nicalon composites. It utilizes an estimation procedure known as the LMN function to derive J-R curve information from load-displacement flexure data in which crack length was not explicitly measured. Results are represented in normalized load vs. normalized plastic displacement plots, J-R curves (J vs. Δa) and comparative J_{Ic} behavior (expressed as equivalent K_{Ic}) as a function of fiber coating thickness.

PREVIOUS EXPERIMENTAL RESULTS

The fabrication of the CVI SiC / Nicalon ceramic matrix composite has been documented elsewhere in detail by Lowden (1989), but essentially entails the slow deposition of ß-phase silicon carbide through chemical vapor infiltration of a reinforcing fabric preform. Miller et al.(1996) observed from experimental data that the flexure strength was significantly affected by changes in the fiber coating (pyrolytic carbon)

thickness ("interlayer thickness") ranging through values of 0, 0.030 μm, 0.060 μm, 0.130 μm, 0.270 μm, 0.580 μm and 1.27 μm (Fig. 1). Individual Nicalon fiber diameter was typically 10 μm and up to 500 fibers were grouped together in tows for the cross-woven fabric. Initial effects from incremental increases in coating thickness were much more pronounced than those observed when the coating thickness exceeded ~0.5 μm. For the case where the Nicalon fibers had no coating, a flexure strength of 85 MPa was observed. This value rose to ~275 MPa for a fiber coating thickness of 0.030 μm, and increased further to ~395 MPa for a coating thickness of 0.060 μm. The maximum flexural strength was observed to be ~420 MPa for a coating thickness of 0.130 μm. Miller et al. then observed flexural strength to decrease to ~330 MPa at a coating thickness of 0.270 μm and to ~275 MPa for a coating thickness of 0.580 μm. Subsequent increases in coating thickness were not observed to have any effect and the asymptotic value of flexure strength for "heavily coated" Nicalon fibers is apparently 275 MPa.

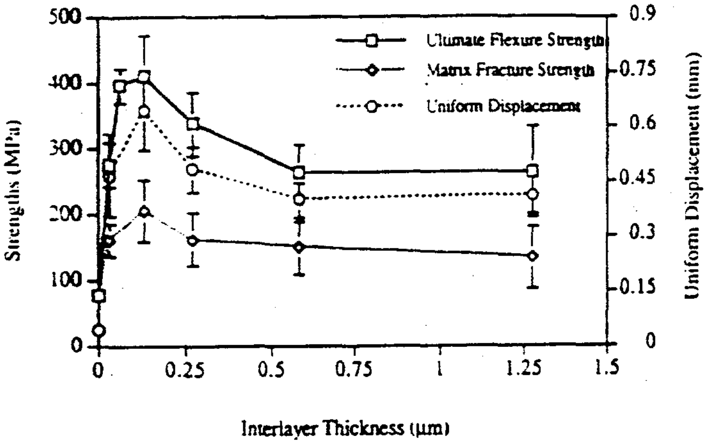

Fig. 1 Ultimate flexure strengths, matrix fracture strengths, and uniform displacements of unnotched specimens (with varying coating thickness) subjected to four point flexure testing (Miller, 1995).

The postulated reason for this fluctuating behavior in flexure strength was attributed to the initial positive influence of fiber coatings in promoting a balance between fiber / matrix friction and debonding /slipping. These positive effects were short-lived as the coating was increased which apparently resulted in loss of good mechanical interaction between the two phases. Beginning with a "no coating" scenario, the bond between the fiber and matrix phases was shown to be too adhesive and strong. Thus as matrix crack initiation and propagation occur, the fiber appears as a continuous phase and cracking tends to drive right through the fiber. This offers no opportunity for the fiber to exercise its higher modulus and strength in mitigating matrix cracks, either through crack bridging, branching, deflection or controlled slippage at the fiber / matrix interface. These same mechanisms explain why the CVI SiC / Nicalon behaves with apparent pseudo-plastic characteristics in fracture toughness evaluations.

Small additions of the pyrolytic carbon coating provide a semi-lubricious sliding interface that permits successful load transfer among fiber and matrix phases, allowing energy to be dissipated from advancing matrix cracks. The macroscopic result is higher flexure strength and apparent toughness. Greater and greater additions of fiber coating thickness have the deleterious effect of softening the interfacial "grip" between the fiber and matrix phases. Miller et al. (1996) speculated that this dimensional "buffering" of the fiber from the residual compressive stresses in the matrix was the root cause of loss of interfacial traction. This permits fibers to pull out and slide against the adjacent matrix too much, so that the positive properties of the fiber reinforcement are not fully realized or are delayed in taking effect until extensive pullout has occurred (yielding undesirable compliance in flexure).

EXPERIMENTAL PROCEDURE

To test the validity of the assumptions about use of J as an appropriate elastic-plastic parameter for these composites, four (4) chevron notched specimens were selected for consideration in the analysis. These specimens were subjected to three-point bending loads but were not broken at the completion of load-displacement data collection. However, significant plastic deformation was observable in all. The four selections represented a cross-cut of coating thicknesses from 0.040 μm, 0.280 μm, 0.510 μm and 0.990 μm. Specimen sides were machined to approximate equal dimensions (5.6 mm x 5.6 mm square, ~50 mm long). One side (at a central location) was V-notched with a diamond saw which inherently left a blunt crack tip. The specimens were put through conventional three-point flexure testing in which load was linearly applied and measured. Additionally, the total displacement was recorded, from which specimen compliance could be derived (by elimination of machine compliance). Finally, the specimens were flat ground down to half-thickness after flexure testing, to expose cracking propagation and features at the tip of the chevron. The low magnification micrograph in Figure 2 reveals the tightly packed striations of woven Nicalon and the apparent high porosity of the CVI-SiC matrix.

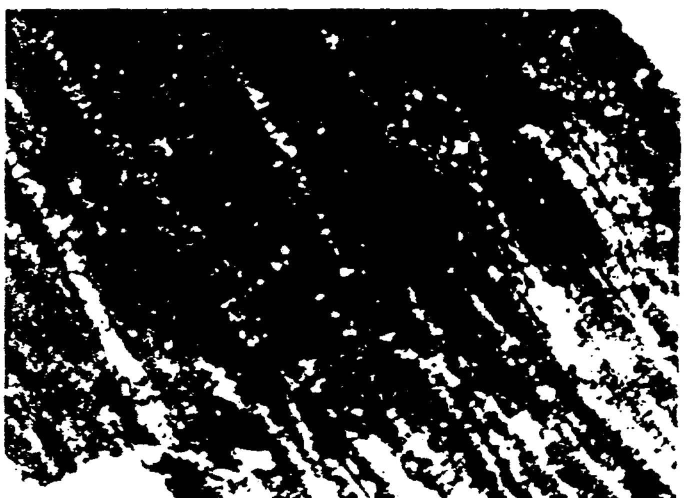

Fig. 2 Optical micrograph of composite with visible Nicalon fibers (bright striations) and residual porosity (dark regions). The ligament from notch root through the specimen is approximately 4.2mm.

The determination of initial (a_o) and final crack length (a_f) was accomplished using optical microscopy with precision-ruled scale bars (on glass slides) inserted into the field of view. It became immediately obvious that the high content of porosity and different phases present in the CVI-SiC challenged the ability to distinguish crack growth. Table 1 lists several representative chevron notch specimens and the observed initial and final crack length information obtained via the described technique. Elastic values such as Young's modulus were taken from flexure test results on unnotched modulus of rupture (MOR) bars with similar coating thicknesses (Miller, 1995).

Table 1. Experimentally Observed Elastic Properties and Crack Growth Information

Spec. ID	Fiber Coat'g Thk (μm)	Elastic Mod. (GPa)	Yield Stress (Mpa)	Poisson's Ratio	a_o (mm)	a_f (mm)
553-4	0.040	110	157	0.174	1.4	3.3
714B-4	0.280	89	165	0.174	1.4	3.9
572-4	0.510	76	146	0.174	1.4	2.8
548-4	0.990	70	130	0.174	0.8	3.6

THEORETICAL MODELING

Observation of the load-displacement data for the chevron-notched specimens indicated the manifestation of "elastic-plastic like" behavior from the fiber reinforcment interacting with the matrix. This prompted consideration of an alternate approach for describing the fracture mechanics of this ceramic matrix composite (CMC) material. Notably, the composite is entirely constituted of brittle materials, yet it exhibits (on a global or macro-scale) apparent ductile behavior (significant plasticity before final failure). Clearly there are a multiplicity of brittle fracture-type mechanisms occurring on the microscale and most previous work on modeling such fracture behavior has recognized the importance of adequately accounting for these mechanisms. However, it is postulated that useful engineering information can be derived from application of existing elastic-plastic fracture mechanics (EPFM) as opposed to complicated models coupling many brittle processes (linear elastic).

Specifically, it is suggested that the J-integral may be a more accurate and appropriate descriptor for characterizing continuous fiber-reinforced ceramic composites. The J integral incorporates elastic strain energy and work of plasticity as a contour integral around the crack tip and quantifies the stress field there. J integral testing is covered in ASTM procedural standards [E 561, E 813, E 1152] which result in a J vs. Δa (incremental crack extension) form. The ASTM standard is rigorous and tedious and requires evaluation of J through one of two different methods. One involves multiple specimen testing with each sample machined to a different initial crack length (a_o). These are then put through similar load / displacement tests and the individual compliance differences are utilized to calculate J. In the other method, a single specimen is subjected to a load-displacement test and at intermediate points the specimen is unloaded to obtain the compliance (which changes with crack growth). An important feature of both tests is the direct and explicit measurement of crack length. The evaluation of the J integral has been reduced to straightforward equations which can be summarized, in principle, as an additive sum of area increments (taken from under the load vs plastic displacement curve). The incremental areas are approximated by a trapeziodal rule. The procedure and the necessary equations are fully described in ASTM E1152 (1987).

With the available CVI-SiC data, the question arises on how to derive meaningful J-information (e.g. J_{Ic} , J-Δa) from the load-displacement (P-v) data taken from the notched bars. Importantly, crack length was not explicitly measured and must be derived from the available data. Accomplishing this required use of fitting techniques (Landes and Herrera, 1988a,b,c; Landes et al, 1991), which sought to model the mixed power law and linear behavior (Fig.3) of the normalized load-plastic displacement curves observed in elastic-plastic materials (usually ductile metals).

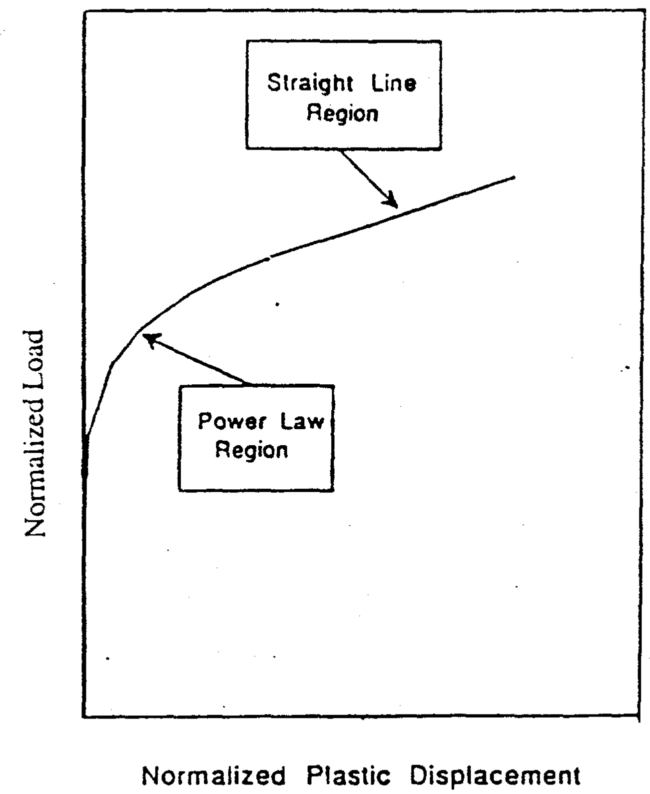

Fig. 3 Power law and linear character of true normalized load-plastic displacement.

In one procedure , Landes and Herrera (1986) treated the load (P) as a separable function of crack length (a) and the plastic portion (v_{Pl}) of the total measured displacement:

$$P = G\left(\frac{a}{W}\right) H\left(\frac{v_{Pl}}{W}\right) \tag{1}$$

The load can then be normalized as:

$$PN = \frac{P}{G\left(\frac{a}{W}\right)} = H\left(\frac{v_{Pl}}{W}\right) \tag{2}$$

The G function may usually be approximated as b^2, where b is the remaining ligament width in the specimen (W-a).

When normalized against a non-growing crack (a_o), the load-plastic displacement curve assumes a shape like that of the physically measured load-displacement curve, since $G(a_o/W)$ is a constant. When crack length is allowed to grow (as actually occurs), then G(a/W) decreases and PN increases. To compensate for physically-observed behavior in most J-R curves, this analysis also employs a modification applied to normalized load values up to P_{max} and seeks to adjust these points for crack blunting behavior. The latter manifests itself in conventional elastic-plastic materials as an apparent crack growth approximately equal to:

$$a = a_o + \frac{J}{2\sigma_Y} \tag{3}$$

where σ_Y is the yield stress.

In Eqn. (3), J can be approximated using the assumption that initial crack length (a_o) does not grow up to P_{max}. The desired blunting adjustment has the effect of raising the normalized load - plastic displacement curve above that obtained when a_o is used throughout. This provides a basis for the power law behavior in the region where (v_{Pl}/W) <<1.

It is known that the total displacement measured consists of an elastic component (v_{El}) and a plastic component (v_{Pl}), such that:

$$v_{Total} = v_{El} + v_{Pl} \tag{4}$$

The elastic component can be simply modeled as a linear function of the compliance C(a/W) which is generally expressed as a polynomial function of the non-dimensionalized crack length (a/W). This analysis used the C(a/W) function for single edge notched bend (SENB) specimens found in Landes et al. (1991). This compliance polynomial assumes a straight-through crack, and it is recognized that more accurate elastic displacement contributions can be obtained with proper compliance expressions for the chevron-notched geometry. The use of chevron-notch bars in evaluating toughness is emerging (Anderson, 1991) and the compliance factors are not presently tabulated as they are for other common test geometries.

Previous work in the field has expressed the resulting normalized load (PN) as a power law, which performs well when (v_{Pl}/W) is very small; but exhibits weakness in the linear portion of observed experimental curves. Landes et al. (1991) sought to employ a fitting function (the LMN Function) which could adequately address the observed behavior in all regions (Fig.4). The LMN function is constructed around three fitting constants (L,M,N) and thus requires three calibration points (labeled A,B,C) to determine their values:

$$PN = \left[L + M\left(\frac{v_{Pl}}{W}\right)\right] \cdot \left(\frac{v_{Pl}}{W}\right)$$

$$= H\left(\frac{v_{Pl}}{W}\right) \cdot \left[N + \left(\frac{v_{Pl}}{W}\right)\right] \tag{5}$$

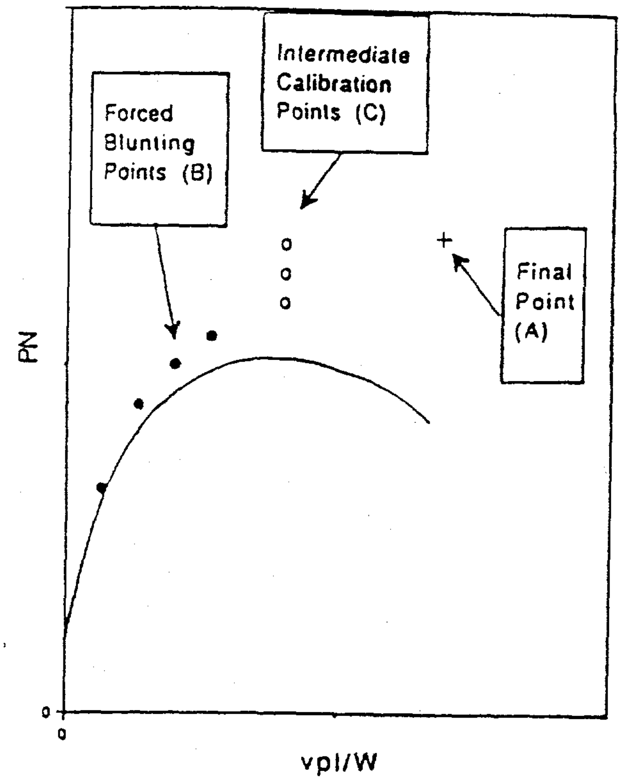

Fig. 4 Schematic of normalization procedure showing three main calibration points.

With pre- and post-examination of known specimens, the initial and final crack lengths, and their associated loads and displacements are known. The final crack length calibration point possesses a significant amount of plastic deformation and will have a corresponding point on the normalized load-plastic displacement curve (A) that is significantly raised above that obtained when a_o is used throughout. This point is the basis for the linear portion which is observed after P_{max} is reached. The forced blunting (B) and intermediate calibration points (C) are iteratively guessed and adjusted to fit the apparent curve. The specific details of the scheme are delineated in Appendix A. Table 2 contains fitting constants derived from this scheme for the four chevron notched specimens.

Table 2. LMN Estimation Fitting Constants Derived for Chevron Notch Specimens

Specimen ID	Fiber Coat'g Thk (μm)	a_o (mm)	a_f (mm)	Fitting Constants L	M (Mn/m2)	N (Mn/m2)
553-4	0.040	1.4	3.3	18.8	322	0.001
714B-4	0.280	1.4	3.9	14.6	368	0.00001
572-4	0.510	1.4	2.8	16.9	71.3	0.0
548-4	0.990	0.8	3.6	14.5	115	0.01025

DISCUSSION OF RESULTS

Figure 5 is the as-collected load cell - load line displacement information from a three point flexure test of Specimen 553-4 (0.040 μm coating thickness). Figure 6 illustrates the normalized load [PN, as computed using $G(a_o/W)$] versus normalized plastic displacement (v_{pl}/W) for Specimen 553-4. This figure also contains the final crack length point computed using a_f and plotted for ease in determining the LMN approximation fitting constants (also shown). Figure 7 consolidates the generated J vs. Δa (or J-R curves) for the four specimens listed in Table 2.

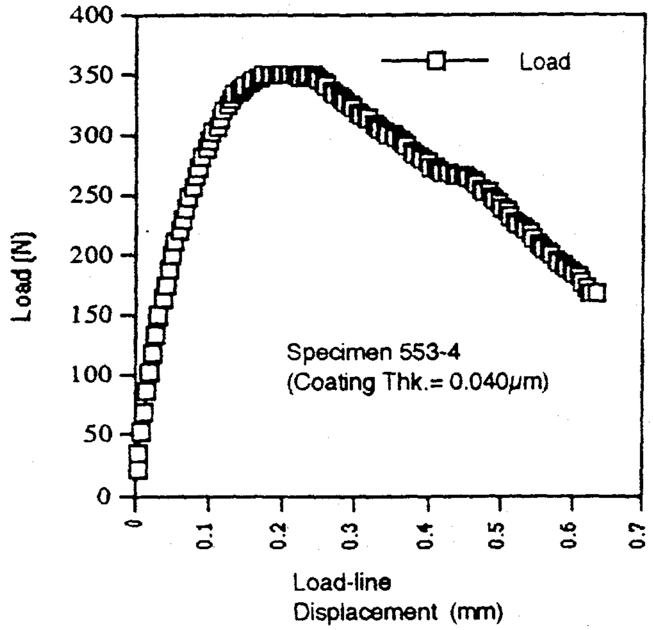

Fig. 5 Representative load vs load-line displacement curve as observed.

The most important result of this analysis is that the J-R data appear to produce moderately rising curves for the smallest coating thicknesses and flatter curves for the thicker coatings (Fig.7). This is indicative of enhanced plasticity (or pseudo-plasticity) for the specimens with the thinner pyrolytic carbon coatings. The effect of such enhanced plasticity is in the higher apparent toughness of these specimens. By contrast, the thicker coating J-R curves indicate a plateau in the J values beyond some critical point. Logically, these specimens would fail more like brittle materials with less dissipation of fracture energy prior to failure.

In all cases, the linear upper portion of the J-R curve can be extrapolated back to the ordinate to obtain a J_{Ic} approximation. More importantly, this value can be converted to a purely elastic component for comparison with similar data. This comparison provides the essential answer to the stated objective of determining the appropriateness of using J over K for these CMC materials.

The formula for the elastic conversion is:

$$K_{Ic_{equiv}} = \sqrt{J_{Ic} \cdot \frac{E}{\left(1 - \nu^2\right)}} \qquad (6)$$

where E is the elastic modulus and ν is the Poisson's ratio for CVI-SiC / Nicalon composites (Table 1). Table 3 shows the elastic values used, their source from unnotched specimen flexure tests and the corresponding equivalent K values computed from J_{Ic} for the chevron notched specimens. The latter tend to be 25-50% higher than the linear model-derived K values. This is somewhat expected since a broader consideration of plastic effects has been pursued. The importance of the finding is that the current practice of using K values may significantly underestimate the engineering toughness of the material.

Table 3. Comparison of Linear Model Derived K (Miller, 1995) versus Equivalent K (from J_{Ic})

Unnotched Specimen	Coating Thk. (μm)	K_{Ic} (MPa$\sqrt{m}$)	Chev. Notch Spec.	Coating Thk. (μm)	J_{Ic} Obs'd (N/m)	Equiv. K_{Ic} (MPa$\sqrt{m}$)
526-4	0.030	12.65	553-4	0.04	2985	18.4
524-4	0.270	12.3	714B-4	0.280	2652	15.6
525-4	0.580	10.58	572-4	0.510	2101	12.83
521-4	1.270	9.92	548-4	0.990	2700	13.96

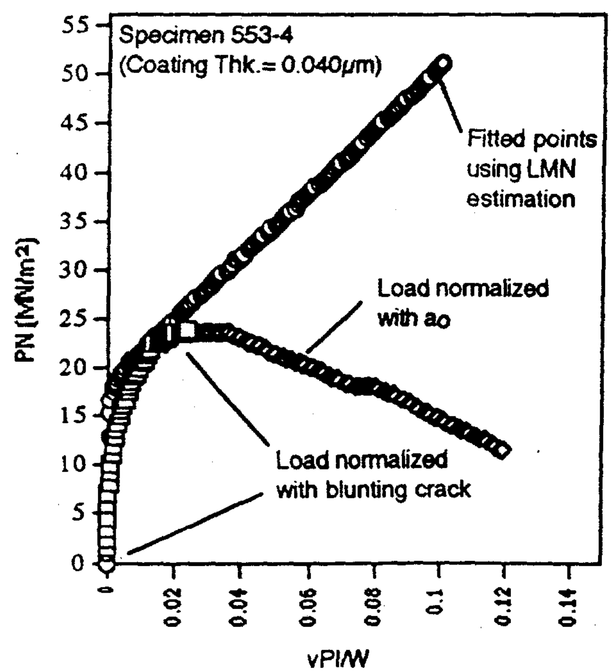

Fig. 6 Normalized load vs plastic displacement data and LMN approximation.

It should be cautioned that the model exhibited some sensitivity to the crack length values used in it (initial and final). The ability to distinguish and determine these from the micrographs of the material structure proved difficult and there is some unquantified uncertainty.

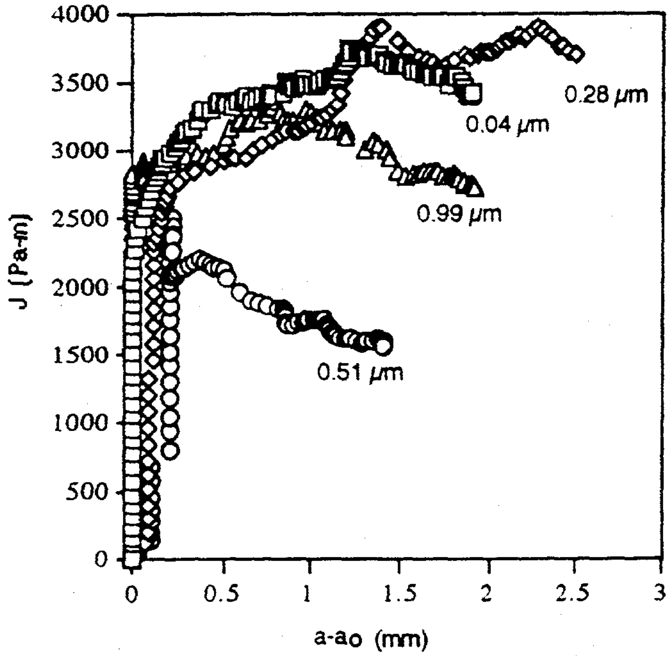

Fig. 7 Derived elastic-plastic fracture toughness (J) vs. crack growth (a-a_0) curves for specimens with different coating thicknesses.

CONCLUSIONS AND RECOMMENDATIONS FOR FUTURE WORK

A CFCC material (CVI-SiC / Nicalon) has been evaluated as elastic - plastic in a fracture toughness assessment. The assessment was performed using only load cell and load line displacement data gathered in three point flexure testing. The unbroken specimens were sectioned to reveal crack growth from the loading. Coupled with initial crack length and the load-displacement information, an estimation procedure was employed for generating the necessary crack growth data. The estimation model (LMN function) serves to simulate the widely observed behavior of tough metals when expressed as normalized load - normalized plastic displacement. Further it permits computation of the J integral, so that J-R curves can be synthesized. The curves which resulted from this analysis revealed credible material responses that paralleled ductile metals in their toughness.

It is speculated that the global result of many different brittle fracture and fiber interface mechanisms is somewhat analogous to the effects of slip systems in metals in interpreting the toughness of the material. This is not a particularly significant conclusion in that the consideration can only be taken at the macro-scale. Certainly, the physical phenomena that give rise to crack-tip plasticity in metals are far removed from the brittle micromechanisms in CMC's. The physical meaning of "crack length" for such diversely branched fracture behavior, remains a difficult problem.

The apparent toughness values from this material are comparatively low (~ 20 Mpa√m) and indicate a need for more work in deriving full strengthening / toughening from the fiber reinforcement. From the same perspective as the Miller study and model, the optimal fiber coating thickness effect (for toughening) appears to be less than 0.10 μm. This was evidenced by the rising J-R curve for the 0.40 μm coating thickness specimen. Such behavior illustrates significant "plasticity" occurring prior to failure.

This study has demonstrated that such materials as the CVI-SiC / Nicalon can be successfully described using EPFM (J). Certainly, better approximations to actual J or equivalent K values can result from a correct ASTM treatment (i.e. notched specimens with crack length monitoring). Alternately, new ASTM standards could be derived from such experiments which would better suit these materials. As a further recommendation, additional studies should seek similar avenues for providing usable data for designers and others who employ these materials in their products. Future work is suggested to investigate fatigue behavior in the CVI-SiC / Nicalon composite.

REFERENCES

Anderson, T.L., 1991, *Fracture Mechanics: Fundamentals and Applications*, CRC Press, ISBN 0-8493-4277-5, pp. 521-524.

ASTM Standard Test Method for Determining J-R Curves, 1987, ASTM E 1152-87.

Landes, J.D. and Herrera, R., 1988a, "A New Look at J-R Curve Analysis", International Journal of Fracture, #36, pp.R9-R14, .

Landes, J.D. and Herrera, R., 1988b, "Calculation of J from Test Records for the Growing Crack", International Journal of Fracture, #36, pp.R15-R20.

Landes, J.D. and Herrera, R., Sept. 1988c, "A Direct J-R Curve Analysis of Fracture Toughness Tests", Journal of Testing and Evaluation (JTEVA), American Society for Testing and Materials, Vol.16, No.5, pp.427-449.

Landes, J.D., Zhou, Z., Lee K., and Herrera, R., July 1991, "Normalization Function for Developing J-R Curves with the LMN Function", Journal of Testing and Evaluation (JTEVA), American Society for Testing and Materials, Vol.19, No.4, pp.305-311.

Lowden, R.A., March 1989, "Characterization and Control of the Fiber -Matrix Interface in Ceramic Matrix Composites", ORNL / TM-11039, Oak Ridge National Laboratory, Oak Ridge, TN.

Miller, J.H. , December 1995, "Fiber Coatings and the Fracture Behavior of a Woven Continuous Fiber Fabric -Reinforced Ceramic Composite", Master's Thesis, The University of Tennessee, Knoxville,TN.

Miller, J.H., Lowden, R.A. and Liaw, P.K., 1996, "Effects of Fiber Coating Thickness on Fracture Behavior of Continuous Woven Fabric-Reinforced Ceramic Composites", (to be published in *Acta. Metall.*)

Appendix A

The progressive nature of these steps was modeled on an Excel spreadsheet. The order of steps is;

1) From P,v data pairs and a_o, generate $C(a_o/W)$
2) Calculate $v_{El} = P^* C(a_o/W)$
3) Calculate v_{Pl} by difference ($=v_{Total} - v_{El}$)
4) Normalize as v_{Pl}/W (where W is specimen width in notch direction)
5) Calculate $G(a_o/W)$
6) Calculate $PN = P/ G(a_o/W)$
7) Plot PN vs v_{Pl}/W
8) Enforce blunting up to P_{max}, by growing crack length a:
   $$a = a_o + \frac{J}{2\sigma_Y}$$
9) J is evaluated tentatively based on vPl using a_o
10) Plot new PN (using blunted "a" values), and plot (PN, v_{Pl}/W) point using a_f
11) Estimate L,M,N values that yield linear behavior between P_{max} and a_f points (i.e. L is y-intercept and M is slope)
12) Express PN as Eqn. 5 and as Eqn. 2
13) Iterate on "a" values until PN's in Step 12 match
14) Continue for all points until each P,V data pair has a corresponding "a"
15) Proceed with computation of J, $\Delta a = a-a_o$; and plot as J-R curves.